Hindawi
Journal of Mathematics
Volume 2023, Article ID 8413894, 8 pages
https://doi.org/10.1155/2023/8413894

Research Article

Application of PDE Constrained Optimization in Internal Combustion Engine Pollution Control

Hongliang Guan

Jilin Railway Technology College, Jilin, China

Correspondence should be addressed to Hongliang Guan; 1600564@qq.com

Received 31 July 2022; Revised 1 January 2023; Accepted 10 January 2023; Published 2 February 2023

Academic Editor: Kenan Yildirim

Aiming at the problem of secondary pollution of waters due to the difficulty of controlling the dosage of purifiers in the treatment of internal combustion engine pollution, a partial differential equation (referred to as PDE) constrained optimization algorithm based on l^1-norm is proposed. The algorithm first converts the internal combustion engine control model of the scavenger dose into a constrained optimization problem with a l^1-penalty term. Secondly, it introduces a dose constraint condition based on PDE and uses the inherent property of Moreau-Yosida regularization to establish a smooth minimization function. Finally, the semismooth Newton method is used to iteratively find the optimal solution. The results of the comparison experiment show that the algorithm in this paper has a great improvement in the results of Newton step number and dose area percentage.

1. Introduction

In recent years, behind the rapid development of the marine economy, the state of the marine environment is not optimistic, and it is facing unprecedented challenge, and seawater pollution is the most important manifestation of marine environmental pollution [1]. Seawater pollutants have many species, a wide range of pollution, and a large impact effect, which has attracted more and more attention at home and abroad. Therefore, researching the optimal dosage of purifiers is the top priority in the treatment and control of internal combustion engine pollution, which is of great significance for the protection of the marine ecological environment and the safe management of water resources [2].

Owing to realize the pollution-free management of the ocean, Lavaei and Lavaei et al. [3] proposed a comprehensive analysis method based on neural network and genetic algorithm. The algorithm can calculate the concentration of pollutants in different times and does not require the use of complex mathematical formulas. However, it only plays a role in local water pollution and cannot solve the large-scale pollution problem. In order to expand the scope of purification, Rivard et al. [4] combined the finite element algorithm and the optimal control theory into an optimal control analysis method suitable for water pollution. The method effectively controls the concentration of pollutants in water by adjusting the inflow speed of the river, which plays a role in controlling marine pollution in a vast range, but it can only control water pollution in a short period of time and cannot be used as a long-term method [5]. Combining the above two algorithms, they have some deficiencies in the governance of marine pollution, and a more efficient algorithm is needed to solve the problem of internal combustion engine pollution.

PDE constrained optimization is an optimization control problem based on PDE constraint, which is usually applied in many fields, such as engineering and science [6]. In recent years, the control method of PDE constrained optimization has received extensive attention in the medical field, whose calculation process mainly has two stages. First, it uses the physical models to reconstruct medical images, whose reconstruction process can be expressed as a constrained optimization problem [7]. Secondly, the physical formula of dose deposition is introduced by precomputing the partial differential equation of fascicle discretization, but this simplified dose calculation is prone to large errors. In addition, it also requires high computational cost, which

means that more efficient optimization algorithms are needed to overcome these difficulties under the constraints of state variables [8]. There are many feasible methods, among which the gradient descent method and Newton method are the two most commonly used optimization methods [9]. For the gradient descent method, its optimization thought is to use the negative gradient direction as the search direction, so that the objective function to be optimized is gradually decreased, which implies the solution does not guarantee a global optimal solution [10]. However, the Newton method is an optimization algorithm that approximates solving equations in the real and complex field, and each iteration of it requires solving the Hessian matrix of the objective function Inverse matrix, which makes the calculation more complicated [11, 12].

As the difficulty of solving PDE optimization problems increases, researchers have developed a series of optimization methods to deal with the problem. An effective method is to add l^0-norm or l^1-norm as a penalty term in the objective equation, but the objective equation based on l^0-norm is not easy to solve and the computational cost is too large, so this paper chooses the l^1-norm penalty term. In 2017, Barnard et al. [14] proposed a PDE-constrained optimization algorithm based on l^1-norm for the PDE optimization problem of radiotherapy. First, all inequality constraints were integrated as integral forms into the objective function of the original problem, then the smoothing techniques were used to burnish the nonsmooth penalty items, and finally the semi-smooth Newton method was used to solve [14]. Inspired by this method, this paper introduces the PDE's l^1-norm constraint optimization algorithm into the marine pollution control. Adjusting the dose limiting conditions by constraining the target area and risk area point by point, the l^1-norm penalty term was used to reconstruct the optimization function of the objective function. Compared with the control variable parameterization method (CVP) [15], this algorithm has a better numerical effect, and it guarantees that the dosage of the purifier is minimized under the condition of not exceeding the desired level, effectively controlling marine pollution and optimizing the living environment of marine life.

In summary, the main contributions of our work are as follows:

(i) We propose a partial differential equation optimization algorithm (PDE) based on l^1 norm, which is applied to the water pollution control of internal combustion engines to achieve the combination of physical control and mathematical drive.

(ii) In our method, dose constraint conditions based on PDE are introduced and actual numerical experiments are carried out on this basis.

(iii) Compared with the traditional method CVP, we have greatly improved the convergence and the proportion of dose area, and also used in the practice waters to further verify the effectiveness of this method.

We review the background theory in the second section and gave the model of internal combustion engine pollution control. In the third part, based on the physical model of l^1-norm, the optimization problem with affine operator as the core is established. Then, in the fourth part, the semismooth Newton method is used for numerical solution. In the fifth part, we use different parameter thresholds to compare different methods, which proved the effectiveness of this method in internal combustion engine pollution control. Finally, the sixth part puts forward the conclusion and future prospects.

2. Background Theories

First of all, assuming stable flow in the sea area, the average flow velocity is 0.125 cm\s, the density of pollutants is more than the water, and its diffusion speed is affected by the wind; the coefficient of wind drift is 0.03; reaction rate constant, longitudinal dispersion coefficient, transverse dispersion coefficient, and net surface tension coefficient of the purification agent, respectively, are 0.02 km\h, 1.35 cm^2\s, 0.45 cm^2\s, and 0.03 N\m [5]. Starting with the center to release the purifier in the polluted area, the purifying agent emission not only needs to consider the general flow state of the ocean current, but also must ensure that the dosage of the purifier reduces the secondary pollution of the water source while eliminating pollution; thereupon, we can establish purification agent reaction diffusion equation as follows [5]:

$$\begin{cases} y_t = m\Delta y + k_{wc}u, \\ y(x,0) = 0, \\ y(0,t) = b, \\ y(\infty,t) = 0. \end{cases} \tag{1}$$

Equation (1) can be abbreviated as $\varepsilon(y,u)$, where y is the dose of the existing scavenger, t is the time state variable, x is the range of the risk or target area, $m\Delta y$ is the diffusion term of the purifiers, $m\,(m>0)$ is the diffusion coefficient of the movement of water molecules, generally in between 0.12~0.34 $cm^2\,s^{-1}$, $\Delta y = \sum_{i=1}^{N} \partial^2 y/\partial^2 x^2$ represents the Laplace operator, $k_{wc}u$ is the reaction term of the purifiers, u represents the dose of purifiers added, k_{wc} represents an embedded map from $L^2(0,T;L^2(wc))$ to $L^2(0,t;L^2(\Omega))$, and $\Omega \subset R^n$ is all waters.

Secondly, according to the constraints of the dose of the purifiers, the dose of the purifiers should be higher than the dose level U in the target area (contaminated water); contrarily, the dose of the purifiers should be lower than the dose level L in the risk area (unpolluted water), and which satisfy equation (2) as a whole [14], so the optimization problem of marine pollution is as follows:

$$\begin{cases} \min\limits_{u\in V_{ad}, y\in Y} \dfrac{1}{2}\|u\|_V^2 + \dfrac{\alpha}{2}\|y-z\|_{L^2(Q)}^2, \\ \text{s.t}\,\varepsilon(y,u) = 0, \\ C_{\omega T}y \geq U, a.e.in\omega_T, \\ C_{\omega R}y \leq L.\ a.e.in\omega_R. \end{cases} \tag{2}$$

Let C_w: $L^2(0,T;L^1(w)) \longrightarrow L^1(w)$ (where $w = w_R$ or $w = w_T$) denote integral operator, $z \in L^2(0,T;L^2(\Omega))$ is the expected value of the dose of the purifiers.

3. Principle Method

3.1. Optimization Problem. In equation (3), due to the dosage of the purifiers $C_w y$ is continuous; therefore, the target area w_T and the risk area w_R cannot be separated, which makes it difficult to solve the marine pollution model. For this reason, in the case of Lagrange multipliers $\beta_1, \beta_1 > 0$, the l^1-norm is introduced as a penalty term into the following objective equation [16]:

$$\begin{cases} \min\limits_{u \in V_{Aad}, y \in Y} \dfrac{1}{2}\|u\|_V^2 + \dfrac{\alpha}{2}\|y - z\|_{L(Q)}^2 + \beta_1 \displaystyle\int_{w_T} \left| \left(C_{w_T} y - U\right)^- \right|_{L^1(w_T)} \mathrm{d}x + \beta_2 \int_{w_R} \left| \left(C_{w_{TR}} y - L\right)^+ \right|_{L^1(w_R)} \mathrm{d}x, \\ \text{s.t. } \varepsilon(y,u) = 0, \end{cases} \tag{3}$$

where let C_w: $L^2(0,T;L^1(w)) \longrightarrow L^1(w)$ represents the integral operator; $|(C_{w_T} y - U)^-|_{L^1(w_T)}$ denotes l^1-norm in target area w_T ; $|(C_{w_R} y - L)^+|_{L^1(w_R)}$ denotes l^1-norm in risk area w_R.

In order to simplify the objective equation, this paper considers introducing the operator S: $u \longrightarrow y$ in equation (3), and it satisfies the reaction diffusion equation $y_t = m\Delta y + k_{w_C} u$ of the purification agent, then $S = (\partial_t - m\Delta)^{-1} k_{w_C}$, where $\Delta = \partial_{xx}$ and $k_{w_C} u(t,x) = \sum_{i=1}^N x_{wi}(x) u_i(t)$.

Theorem 1. *Operator S is a affine.*

Proof. By $y = Su$, where $y \in Y$, $u \in L^2(0,T;L^2(w_C))$, and for every $u \in V$, there is a unique solution y in partial differential equation $\varepsilon(y,u) = 0$; let $y_t - m\Delta y - k_{w_C} u = 0$, then

$$\int_0^T y_t \mathrm{d}t = \int_0^T (m\Delta y - k_{wc} u)\mathrm{d}t. \tag{4}$$

Since $k_{w_C} u$ is a constant [4], and because $\Delta y = \sum_{i=1}^N \partial^2 y / \partial^2 x^2$, so

$$y + C = mY + k_{wc} uT. \tag{5}$$

Thus, $y = (mY - C) + k_{wc} uT$, where $Y = \int_0^T \sum_{i=1}^N \partial^2 y / \partial^2 x_i^2 \mathrm{d}t$.

According to the definition of affine [16, 17], $(mY - C)$ represents the translation matrix of $u \longrightarrow y$ and $k_{w_C} uT$ represents the transformation matrix of $u \longrightarrow y$, so S is an affine.

Substituting $y = Su$ into equation (3) translates into the following optimization problem:

$$\min_{u \in V_{Aad}} \frac{1}{2}\|u\|_V^2 + \frac{\alpha}{2}\|Su - z\|_{L(Q)}^2 + \beta_1 \int_{w_T} \left| \left(C_{w_T} Su - U\right)^- \right|_{L^1(w_T)} \mathrm{d}x + \beta_2 \int_{w_R} \left| \left(C_{w_{TR}} Su - L\right)^+ \right|_{L^1(w_R)} \mathrm{d}x, \tag{6}$$

where V is the feasible solution set of dose u; let $V \coloneqq L^2(0,T;L^2(w_C))$, for $x \in w_C$, $t \in [0,t]$, exists $V_{ad} = \{u \in L^2(0,T;L^2(w_C)); U_{\min} \le u(t,x) \le U_{\max}\} \subset V$, and $w_C \subset \Omega$ is the observation domain.

For every $\alpha > 0, \beta_1$, and $\beta_2 > 0$, there is a unique minimum value $\bar{u}$ in equation (6), and $\bar{u} \in V_{ad}$ [14]. Literature [14] further discussed the convergence of the solution for β_1 and $\beta_2 \longrightarrow \infty$. Assuming V_{ad} is bounded, there is a subsequence $\{u_n\}_{n \in N}$ that converges to the solution of equation (6).

3.2. Moreau-Yosida Regularization. Since the objective equation based on l^1-norm is composed of the absolute value function [18], it is not differentiable at the origin. In order to solve the state variable u, Moreau-Yosida regularization is needed to burnish the nonsmooth penalty [19]. Firstly, assuming that $\bar{u} \in V_{ad}$ is the minimum value of equation (6), then there exists $\bar{\mu}^+(x) \in L^\infty(w_R)$ and $\bar{\mu}^-(x) \in L^\infty(w_T)$, and the following formula holds:

$$\begin{cases} \bar{u} = \mathrm{prox}_{V_{ad}}(-\bar{p})), \\ \bar{\mu}^+(x) = \partial g^+\left(\left[C_{w_R} s\bar{u}\right](x)\right) \text{for } a.e\, x \in w_R, \\ \bar{\mu}^-(x) = \partial g^-\left(\left[C_{w_T} s\bar{u}\right](x)\right) \text{for } a.e\, x \in w_T, \end{cases} \tag{7}$$

where

$$\begin{aligned} \bar{p} &= S_0^*\left(\alpha(S\bar{u} - z) + \beta_1 \left| \left(C_{w_T} S\bar{u} - U\right)^- \right|_{L^1(w_T)} \mathrm{d}x + 1 \left| \left(C_{w_R} S\bar{u} - L\right)^+ \right|_{L^1(w_R)} \mathrm{d}x, \right. \\ g^+(v_R) &= \left|(v_R - L)^+\right|, g^-(v_T) = \left|(v_T - U)^-\right|. \end{aligned} \tag{8}$$

Then, the regularization factor γ is introduced to equation (9), converting into the following regularization form:

$$\begin{cases} u_\gamma = \text{prox}_{V_{ad}}\left(-p_\gamma\right)\right), \\ u_\gamma^+(x) = \partial g_\gamma^+\left(\left[C_{w_R} S u\right]_\gamma(x)\right) \text{for } a.e\, x \in w_R, \\ u_\gamma^-(x) = \partial g_\gamma^-\left(\left[C_{w_T} s u_\gamma\right](x)\right) \text{for } a.e\, x \in w_T, \end{cases} \tag{9}$$

where

$$\partial g^+(v) = \left(\partial g^+(v)\right)_\gamma(v) \coloneqq \frac{1}{\gamma}\left(v - \text{prox}_{\partial g^+}(v)\right) \text{ and}$$
$$\text{prox}_{\partial g^+}(v) \coloneqq \underset{w \in R}{\text{argmin}} \frac{1}{2\gamma}|w - v|^2 + g^+(w) = \left(Id + \gamma \partial g^+\right)^{-1}(v), \tag{10}$$

are the project mapping of g^+ [14].

4. Implementation Details

Since the objective function (9) is semismooth, its directional derivative always exists, so it can be solved numerically using the semismooth Newton method. The specific steps are as follows:

(1) Let $h_\gamma^+ \coloneqq \partial g_\gamma^+$ and $h_\gamma^- \coloneqq \partial g_\gamma^-$, differentiate h_γ to get the corresponding Newton derivative.

(2) Rewrite the objective equation (9) by eliminating μ_γ^+ and μ_γ^-, then

$$u_\gamma - \text{prox}_{V_{ad}}\left(-S_0^*\left(\alpha\left(Su_\gamma - z\right) + \beta_1 C_{w_R}^* H_\gamma^+\left(C_{w_R} S u_\gamma\right) + \beta_2 C_{w_T}^* H_\gamma^-\left(C_{w_T} S u_\gamma\right)\right)\right) = 0, \tag{11}$$

where $[H_\gamma(y)](x) = h_\gamma(y(x))$.

(3) Establish the reversibility of Newton's step $D_N T(u^k)\delta u = -T(u^k)$, then

$$\left(Id + \chi V_{ad}\left(-F\left(u^k\right)\right) D_N F\left(u^k\right)\delta u = -\left(u^k - \text{proj}_{V_{ad}}\left(-F\left(u^k\right)\right)\right), \tag{12}$$

where

$$F\left(u^k\right) = S_0^*\left(\alpha\left(Su_\gamma - z\right) + \beta_1 C_{w_R}^* H_\gamma^+\left(C_{w_R} S u_\gamma\right) + \beta_2 C_{w_T}^* H_\gamma^-\left(C_{w_T} S u_\gamma\right)\right),$$
$$D_N F\left(u^k\right) = S_0^*\left(\alpha + \frac{\beta_1}{\gamma} C_{w_R}^* \chi^+\left(C_{w_R} S_0 u^k\right) C_{w_R} + \frac{\beta_2}{\gamma} C_{w_T}^* \chi^-\left(C_{w_T} S_0 u^k\right) C_{w_T}\right) S_0. \tag{13}$$

(4) Choose $u^0 \in R^n$; for given u^k, there is $F(u^k) \neq 0$, $V_k \in D_N F(u^k)$, then exists

$$V_k h^k = F\left(u^k\right), \tag{14}$$

if there exists a solution, then it must satisfy $|h^k| \leq b|F(u^k)|$.

(5) After further iteration, if the following formula is satisfied

$$\left|F\left(u^k + h^k\right)\right| < \gamma F\left(u^k\right), \tag{15}$$

then the final state variable u can be determined.

The algorithm G is given as follows:

(1) Initialize $u^0, \beta, \gamma, \sigma, \beta, \gamma \in (0,1)$ and $\sigma \in (0, \bar{\sigma})$, give the maximum number of iterations

(2) Let $k = 0$, 1, 2, ..., n, through equation (14) to calculate h^k

(3) If h^k satisfies equation (15), output u^k, otherwise proceed to the next step

(4) Let $d^k = h^k$, $\alpha^k = 1$, compute $u^{k+1} = u^k + \alpha_k d^k$, go to step (2) until equation (15) is satisfied

In this paper, the convergence of algorithm G is derived from the local Lipschitz continuity and B-differentiable properties [20], $\theta(u) = |F(u)|^2$ define the function θ, and the specific convergence proof can be found in the literature [21, 22].

Table 1: Results for dose-constrained equation (2): number of SSN steps, volume fraction for risk, and target regions for different values of γ.

γ/γ_0	1.25×10^{-1}	3.45×10^{-3}	3.12×10^{-2}	3.91×10^{-3}	1.95×10^{-3}	7.81×10^{-4}
#SSN	1	1	3	15	57	*
% w_R above L	0	0	13.64	13.64	14.79	*
% w_T below U	100	100	100	100	100	*

*Failure to converge.

Table 2: Results for dose-constrained equation (3): number of SSN steps, volume fraction for risk, and target regions for different values of γ.

γ/γ_0	2.50×10^{-1}	2.48×10^{-3}	6.25×10^{-4}	7.81×10^{-6}	3.91×10^{-8}	3.38×10^{-9}
#SSN	1	1	3	3	4	*
% w_R above L	0	0	45.45	45.45	27.12	*
% w_T below U	100	100	93.10	72.96	100	*
#SSN	1	1	3	5	7	27
% w_R above L	0	0	11.63	13.95	13.95	33.80
% w_T below U	100	100	100	88.79	16.38	16.38
#SSN	1	1	2	3	5	9
% w_R above L	0	0	11.63	11.63	13.95	9.30
% w_T below U	100	100	100	100	88.79	12.07
#SSN	1	1	3	11	11	*
% w_R above L	0	0	11.63	10.46	10.46	*
% w_T below U	100	100	100	10.34	10.34	*

*Failure to converge.

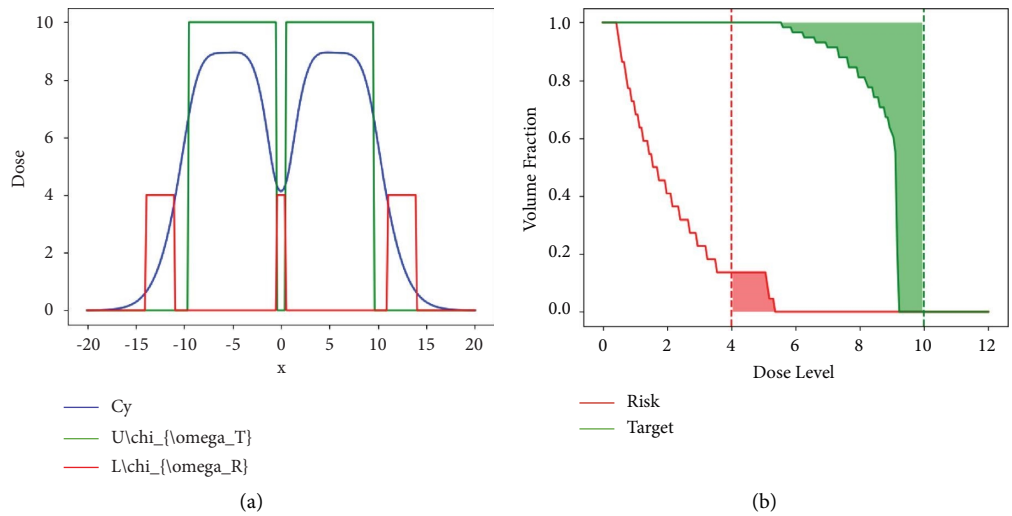

(a) (b)

Figure 1: Dose information for dose-constrained equation (2). (a) Final dose $C_{w_R}y$, risk level L, and target level R. (b) Dose volume histogram for risk w_R and target region w_T.

5. Numerical Example

In order to clarify the effectiveness of the algorithm in this paper, a numerical experiment on the dosage adjustment of the purifiers is performed for the l^1-norm PDE constrained optimization problem, and the experimental results are compared with the CVP method. Given the observation field $\Omega = [-20, 20]$, time $T = 20$, and water molecule diffusion coefficient $m = 0.2$, we choose objective, risk, and control area as w_T: $[-9.5, 9.5]\backslash[-4, 4]$, w_R: $[-14, 11]\backslash[11, 14] \cup [-4, 4]$, and w_C: $[-20, 20]$, respectively. Assuming that $U = 10$, $L = 4$, $U_{\min} = 0, U_{\max} = 20$, and $\alpha = 0$, they represent the Lebesgue measures of the target area and the risk area, respectively. In this paper, the observation area is discretized into 256 spatial nodes and 256 temporal nodes, for equation (2), the initialization γ is γ_0 and $\gamma_0 = 1$; for equation (3), the initialization γ is γ_0 and $\gamma_0 = \max(\beta_1, \beta_2)$, the maximum number of semi-smooth Newton iterations is 400. And in both cases, as long as the semi-smooth Newton method converges, γ and γ_0 will have corresponding changes. The

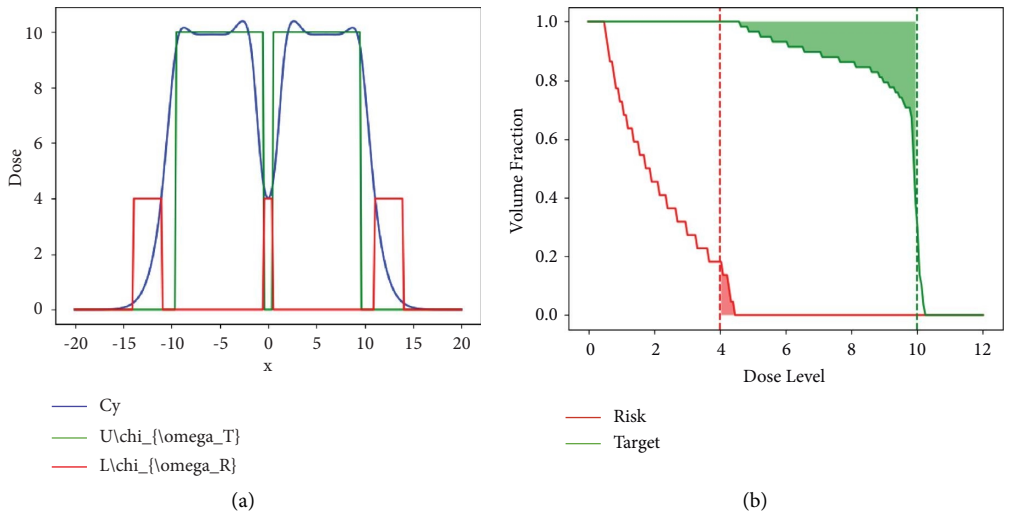

FIGURE 2: Dose information for dose-constrained equation (3) with $\tilde{\beta}_1 = 1.25 \times 10^4$ and $\tilde{\beta}_2 = 1.25 \times 10^6$. (a) Final dose $C_{w_R} y$, risk level L, and target level R. (b) Dose volume histogram for risk w_R and target region w_T.

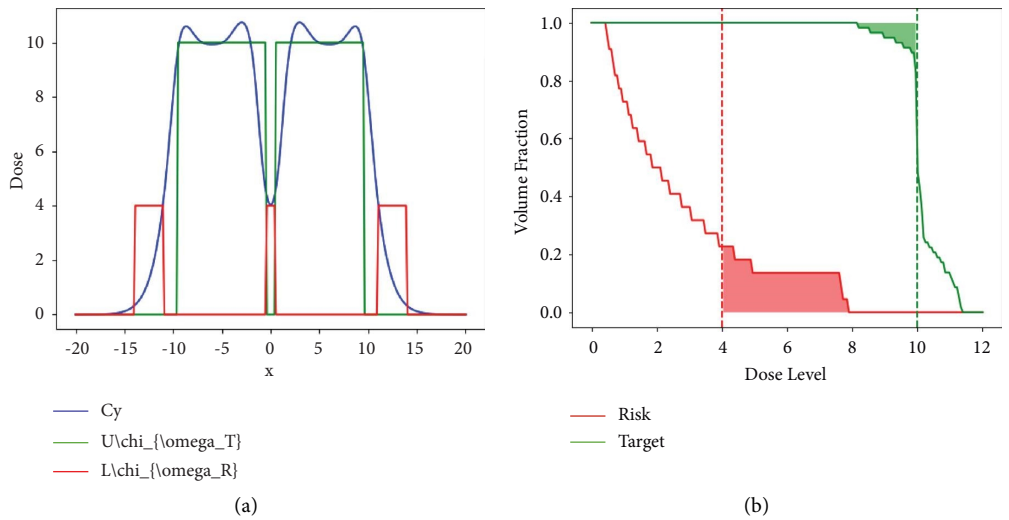

FIGURE 3: Dose information for dose-constrained equation (3) with $\tilde{\beta}_1 = 2 \times 10^4$ and $\tilde{\beta}_2 = 2 \times 10^6$. (a) Final dose $C_{w_R} y$, risk level L, and target level R. (b) Dose volume histogram for risk w_R and target region w_T.

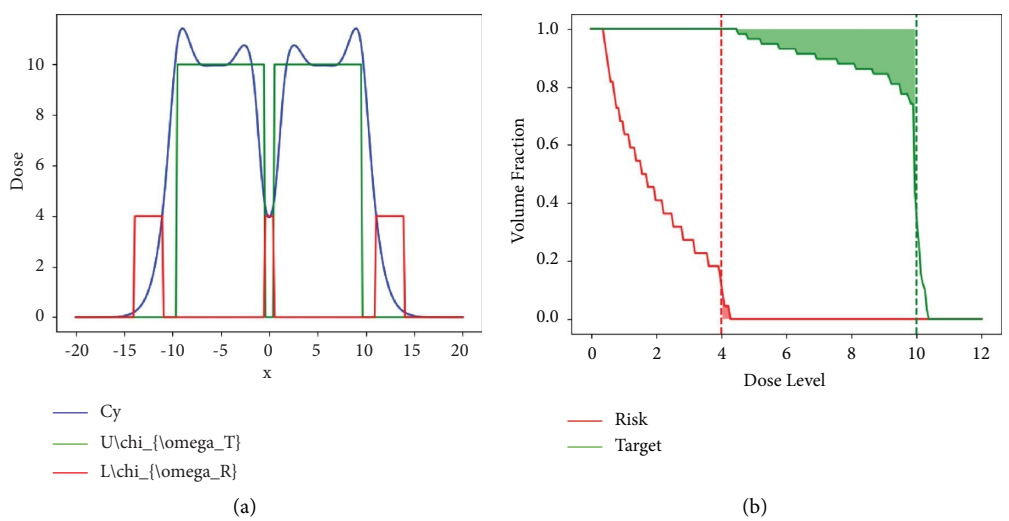

FIGURE 4: Dose information for dose-constrained equation (3) with $\tilde{\beta}_1 = 1.25 \times 10^4$ and $\tilde{\beta}_2 = 2 \times 10^6$. (a) Final dose $C_{w_R} y$, risk level L, and target level R. (b) Dose volume histogram for risk w_R and target region w_T.

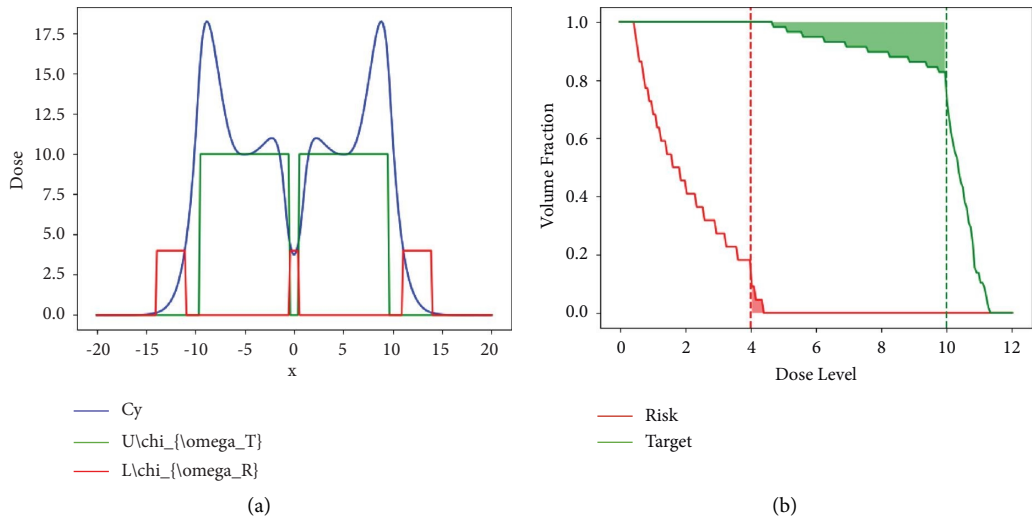

FIGURE 5: Dose information for dose-constrained equation (3) with $\widetilde{\beta}_1 = 2 \times 10^4, \widetilde{\beta}_2 = 2 \times 10^6$. (a) Final dose $C_{w_R} y$, risk level L, target level R. (b) Dose volume histogram for risk w_R and target region w_T.

results of solving equation (2) and equation (9) are given in Figures 1–5, respectively. The dose-volume histogram shows the percentage of the area occupied by w_R and w_T, where the dose C_{w_R} in the risk area is at least 4 and the dose C_{w_T} in the target area is at least 10.

For the solution of the CVP method as shown in Figure 1, for the final value $\gamma \approx 3.62 \times 10^{-3}$, it is found that the numerical solution using this method obviously cannot meet the constraints of the dosage of the purifiers. For all γ, in the target area, the minimum value of the purifiers is samller than U, at the same time, the percentage of the dose above L in the risk area is 16%.

The solution to the PDE's l^1-norm constrained optimization algorithm is shown in Figure 2, let $\widetilde{\beta}_1 = 1.25 \times 10^4$, $\widetilde{\beta}_2 = 1.25 \times 10^6$, and the final value $\gamma/\gamma_0 = 2.28 \times 10^{-6}$, we can find that the effect of the target area is slightly improved, there is 40% w_T with a dose less than U, and the volume fraction of $C_{w_R} y > L$ becomes significantly smaller.

Increase $\widetilde{\beta}_1$ to 2×10^4, while keeping $\widetilde{\beta}_2$ at the value of 1.25×10^6, the final value $\gamma/\gamma_0 = 1.78 \times 10^{-6}$, as shown in Figure 3. It can be found that the target dose coverage has further improved, with a value of 80%; however, the area ratio of risk areas has increased significantly.

Instead, increase $\widetilde{\beta}_2$ to 2×10^6, while keeping $\widetilde{\beta}_1$ at 1.25×10^4, the final value is $\gamma/\gamma_0 = 2.84 \times 10^{-9}$, as shown in Figure 4, the coverage of the area greater than L in the risk area w_R has improved to about 5%, but the area ratio of the target area w_T has reduced to 40%.

Finally, increase $\widetilde{\beta}_1$ to 2×10^4, $\widetilde{\beta}_2$ to 2×10^6, and the final value is still $\gamma/\gamma_0 = 2.84 \times 10^{-9}$, as shown in Figure 5, the area ratio of each area has reached a good effect. Therefore, by adjusting the values of $\widetilde{\beta}_1$ and $\widetilde{\beta}_2$, the dosage of purifying agent in different areas can be balanced better, and it also shows that the PDE constrained optimization algorithm based on l^1-norm can effectively control marine pollution.

In order to better illustrate the advantages of PDE's l^1-norm constraint optimization algorithm, the following table represents the value of γ/γ_0, the number of Newton steps required for the γ, the percentage of the target area w_T below U, the risk area w_R above L, and the percentage of the dose.

The results of the CVP method are given in Table 1. It can be seen that no matter how γ/γ_0 changes, the percentage of the dose in the target area w_T that is lower than U does not change, which shows that the minimum value of the purifiers dose has not reached U, the dose limit condition cannot be met, and it also shows that it is difficult to find a feasible solution between the target area w_T and the risk area w_R. In contrast, Table 2 shows that the optimization algorithm proposed in this paper not only requires fewer iteration steps, but also the percentage of doses higher than L in the risk area w_R is almost unchanged when both $\widetilde{\beta}_1$ and $\widetilde{\beta}_2$ increase to the maximum. The percentage of the dose below U in the target area w_T is also almost unchanged, which proves that the method has good convergence.

6. Conclusion

Despite the rapid development of technologies for controlling internal combustion engine pollution, it is still a major problem in this field to find the optimal amount of purifiers [23–27]. Aiming at the above problems, this paper proposes a l^1-norm PDE constrained optimization algorithm. This algorithm introduces l^1-norm penalty term in the optimal control of purifiers dosage. Using the properties of convex analysis to prove the existence and uniqueness of the optimal solution in the objective equation, at the same time, according to the definition of the adjacent operator, a regularized representation of the target equation is constructed, and finally, the semismooth Newton method is used to obtain the numerical solution. The results of the numerical experiments show that the algorithm in this paper reduces pollution while reducing the diffusion of purification agents and effectively controls internal combustion engine pollution. This proves that the PDE constrained optimization algorithm based on l^1-norm is an effective

method for controlling the dosage of purification agents. In the future, the algorithm can be further refined to adapt to other optimization problems.

Data Availability

The float data used to support the findings of this study are included within the article.

Conflicts of Interest

The author declares no conflicts of interest.

Acknowledgments

This study was supported by the Innovation and practice of pre-qualified personnel training mode for railway locomotive and vehicle manufacturing and maintenance specialty by Jilin Higher Education Association: JGJX2019D705.

References

[1] F. Chuah, K. Mokhtar, A. Bakar et al., "Marine environment and maritime safety assessment using port state control database," *Chemosphere*, vol. 304, Article ID 135245, 2022.

[2] A. L. Lusher, A. Burke, I. O'Connor, and R. Offiffifficer, "Microplastic pollution in the northeast atlantic ocean: validated and opportunistic sampling," *Marine Pollution Bulletin*, vol. 88, no. 1-2, pp. 325–333, 2014.

[3] S. Lavaei and N. Lavaei, "Modelling nitrate pollution of groundwater using artificial neural network and genetic algorithm in an arid zone," *International Journal of Water*, vol. 5, no. 2, pp. 194–203, 2009.

[4] M. J. Rivard, H. R. Ghadyani, A. D. Bastien, N. N. Lutz, and J. T. Hepel, "Multi-axis dose accumulation of noninvasive image-guided breast brachytherapy through biomechanical modeling of tissue deformation using the finite element method," *Journal of Contemporary Brachytherapy*, vol. 1, no. 1, pp. 55–71, 2015.

[5] D. Todescato, F. V. Hackbarth, P. J. Carvalho, A. A. Ulson de Souza, J. Vtor, and P. Vilar, "Correction to: use of cork granules as an effffective sustainable material to clean-up spills of crude oil and derivatives," *Environmental Science and Pollution Research*, vol. 27, no. 1, 2019.

[6] L. Afraites, A. Hadri, L. Laghrib, and M. Nachaoui, "A weighted parameter identification PDE-constrained optimization for inverse image denoising problem," *The Visual Computer*, vol. 38, no. 8, pp. 2883–2898, 2022.

[7] A. Mang, A. Gholami, C. Davatzikos, and B. Biros, "PDE-constrained optimization in medical image analysis," *Optimization and Engineering*, vol. 19, no. 3, pp. 765–812, 2018.

[8] R. Herzog, G. Stadler, and G. Wachsmuth, "Directional sparsity in optimal control of partial differential equations," *SIAM Journal on Control and Optimization*, vol. 50, no. 2, pp. 943–963, 2012.

[9] R. E. J. Schnurr, V. Alboiu, M. Chaudhary et al., "Reducing marine pollution from single-use plastics (sups): a review," *Marine Pollution Bulletin*, vol. 137, pp. 157–171, 2018.

[10] P. Yun and S. Yun, "Block-coordinate gradient descent method for linearly constrained nonsmooth separable optimization," *Journal of Optimization Theory and Applications*, vol. 140, no. 3, pp. 513–535, 2009.

[11] B. Biros and O. Ghattas, "Parallel Lagrange--Newton--Krylov--Schur methods for PDE-constrained optimization. Part II: the Lagrange--Newton solver and its application to optimal control of steady viscous flows," *SIAM Journal on Scientific Computing*, vol. 27, no. 2, pp. 714–739, 2005.

[12] F. Ahmad, E. Tohidi, and J. A. Carrasco, "A parameterized multi-step Newton method for solving systems of nonlinear equations," *Numerical Algorithms*, vol. 71, no. 3, pp. 631–653, 2016.

[13] M. Herty and M. Herty, "The smoothed-penalty algorithm for state constrained optimal control problems for partial differential equations," *Optimization Methods and Software*, vol. 25, no. 4, pp. 573–599, 2010.

[14] R. C. Barnard and C. Clason, "l^1 penalization of volumetric dose objectives in optimal control of PDEs," *Computational Optimization and Applications*, vol. 67, no. 2, pp. 401–419, 2017.

[15] X. Anke, Y. Q. Hu, and X. G. Liu, "Penalty function method for optimal control problem with inequality path constraints," *Journal of Automation*, vol. 1, no. 151, pp. 260–291, 2013.

[16] L. Lubkoll, A. Schiela, and M. Weiser, "An affine covariant composite step method for optimization with PDEs as equality constraints," *Optimization Methods and Software*, vol. 32, no. 5, pp. 1132–1161, 2016.

[17] R. Goebel and R. T. Rockafellar, "Local strong convexity and local lipschitz continuity of the gradient of convex functions," *Journal of Convex Analysis*, vol. 15, no. 2, 2008.

[18] B. A. Turlach, "On Algorithms for Solving Least Squares Problems under an L1 Penalty or an L1 constraint," in *Proceedings of the American Statistical Association*, Statistical Computing Section (CD-ROM), pp. 2572–2577, 2005.

[19] B. Wu, C. Ding, D. Sun, and K.-C. Toh, "On the moreau--yosida regularization of the vector k-Norm related functions," *SIAM Journal on Optimization*, vol. 24, no. 2, pp. 766–794, 2014.

[20] H. H. Bauschke and P. L. Combettes, *Convex Analysis and Monotone Operator Theory in Hilbert Spaces*, Springer, New York, NY, USA, 2011.

[21] K. Kunisch and K. Kunisch, "Semi-smooth Newton methods for state-constrained optimal control problems," *Systems and Control Letters*, vol. 50, no. 3, pp. 221–228, 2003.

[22] H. Florez and M. Arg´aez, "A reduced-ordergauss-Newton method for nonlinear problems based on compressed sensing for PDE applications," in *Nonlinear Systems - Modeling, Estimation, and Stability*InTech, London, UK, 2018.

[23] N. Parikh and S. Boyd, *Proximal Algorithms*, Foundations and trends® in Optimization, vol. 1, no. 3, pp 127–239, 2014.

[24] W. A. Wurtsbaugh, H. W. Paerl, and K. D. Walter, "Nutrients, eutrophication and harmful algal blooms along the freshwater to marine continuum," *Wiley Interdisciplinary Reviews: Water*, vol. 6, no. 5, Article ID e1373, 2019.

[25] I. T.-V. Wysocki and P. L. Billon, "Plastics at sea: treaty design for a global solution to marine plastic pollution," *Environmental Science and Policy*, vol. 100, pp. 94–104, 2019.

[26] T. Rees, H. S. Dollar, and A. J. Wathen, "Optimal solvers for PDE-constrained optimization," *SIAM Journal on Scientific Computing*, vol. 32, no. 1, pp. 271–298, 2010.

[27] D. P. Surowiec and T. M Surowiec, "Existence and optimality conditions for risk-averse pde-constrained optimization," *SIAM/ASA Journal on Uncertainty Quantification*, vol. 6, no. 2, pp. 787–815, 2018.